Observation of Forward Raman Scattering in Laser-Produced Plasmas

R. E. Turner, Kent Estabrook, R. P. Drake, E. A. Williams, H. N. Kornblum, W. L. Kruer,
and E. M. Campbell

Lawrence Livermore National Laboratory, University of California, Livermore, California 94550
(Received 6 June 1986)

We report the first observation of up-shifted scattered light from Raman forward scattering. Computer simulations show this scattering to be a characteristic signature of that instability. The up- and down-shifted spectra are in good agreement with the interpretation of anti-Stokes and Stokes waves, respectively. We have correlated the observations of both the up-shifted and down-shifted forward spectra with the theoretically expected superhot electrons. The experiments used the Nova laser facility to irradiate thin CH targets with 1-nsec pulses of 0.53-μm light.

Raman scattering[1-7] (SRS) in laser-produced plasmas can generate high-energy electrons, which can degrade laser-fusion target gain. Raman forward scattering (RFS) can, in principle, produce very energetic electrons (>1 MeV) and has been suggested[8] as a mechanism to be used in novel electron accelerators for high-energy particle research. Raman scattering is the parametric decay of a laser light wave into a scattered electromagnetic wave and an electron plasma wave. The process obeys the frequency- and wave-number-matching equations $\omega_o = \omega_s + \omega_{epw}$ and $\mathbf{k}_o = \mathbf{k}_s + \mathbf{k}_{epw}$, where the subscripts o, s, and epw refer to the laser, scattered wave, and electron plasma wave, respectively. For forward scattering, all k's are positive resulting in a small k_{epw} with a correspondingly large phase velocity ω_{epw}/k_{epw}. Since the plasma wave accelerates electrons to approximately this velocity,[7] the superhot temperatures are of order 100 keV at the highest possible density (quarter critical), and increase as the density decreases.

Raman forward scattering is a convective instability, whose threshold and gain are generally determined by variations in the plasma density. To minimize the gradients, our plasmas were produced by laser irradiation of a thin foil, which expands with an approximately parabolic density profile through the densities of interest. For a parabolic density profile $n/n_c = (n_p/n_c)[1 - (x/L)^2]$, the gain is given by[9]

$$G = \exp(7[\gamma_0/K''^{1/3}(v_1v_2)^{1/2}]^{3/2}),$$

where γ_0 is the growth rate of the instability, v_1 and v_2 are the group velocities of the scattered light wave and the plasma wave, and K'' is the second derivative of the wave-number mismatch due to the density variation. K'' is determined by the curvature length which, in these experiments, we expect to be limited by the finite spot size. The growth can be reduced[10] if the plasma wave is collisionally damped. However, for our experiments, the damping length is much greater than the growth length; i.e., $v_1/v_{ei} \gg (v_1v_2)^{1/2}/\gamma_0$, and

this reduction does not apply.

It has been previously pointed out[7] that the small value of k_{epw} in forward scattering results in a near-resonant condition for the generation of up-shifted (anti-Stokes) ($\omega_s = \omega_o + \omega_{epw}$) light. Observation of this light in the forward direction provides a signature of RFS that is free from the ambiguities due to refraction or reflection which may be present when one observes the usual down-shifted (Stokes) scattering.

Figure 1(a) shows particle-in-cell simulation[7] results for the fraction of the light Raman scattered forward from a parabolic density profile. In these simulations, the length was fixed at 68 μm, and the peak density and parabolic scale length L (defined earlier) were varied, as shown in the figure and caption. The laser intensity was 4×10^{15} W/cm^2, the wavelength 0.53 μm, and the electron temperature 1 keV, and the ions were fixed. Note that the decrease in RFS at the highest density is due to the small value of L used in this simulation. The gain coefficient inferred from these simulations is in reasonable agreement with Eq. (1),
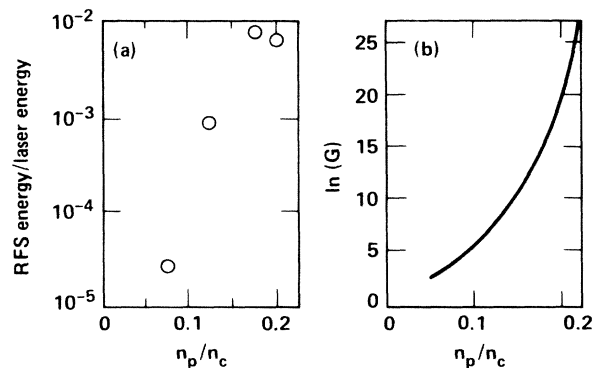
FIG. 1. (a) Fraction of laser energy in Raman forward scattering, from fixed-length computer simulations (see text). Values of parabolic scale-length parameter L are 42, 54, 64, and 48 μm (left to right). (b) Forward Raman gain G calculated for estimated experimental parameters.

typically within about 30% of the theoretical prediction. The fraction of the forward-scattered light shifted upward in frequency in these simulations varied, being typically 15%–25% of the total forward-scattered energy. This fraction depends on the (nonlinear) plasma-wave damping coefficient, and will be discussed later. For our experiments, we can simply estimate the axial density full width at half maximum by setting it equal to the spot size $(2R)$, or $L = \sqrt{2}R$ for the parabolic equation above. Taking $2R = 240$ μm, $I = 4 \times 10^{15}$ W/cm^2, and $T = 2$ keV,[6] we find $G = \exp(20)$ for $n/n_c = 0.2$, while $G = \exp(6)$ for $n/n_c = 0.1$, as plotted in Fig. 1(b). Note that the gain expected at the higher densities should be quite sufficient to produce detectable signals, even with quite small noise levels.

It should be noted that enhanced noise levels are possible when the plasma waves due to SRS backscattering propagate to higher density.[11] Since their wave numbers decrease as the density increases, they can become resonant for the RFS process. This mechanism is quite sensitive to linear and nonlinear damping of the plasma wave, and has been difficult to isolate in the simulations. However, this effect may play a role in helping to explain the observed RFS spectra, which we discuss later.

For these experiments, one arm of the Nova[12,13] laser was used to illuminate a 2-μm-thick CH foil with 2000 J of light at 4×10^{15} W/cm^2 in a 240-μm diameter spot. The incident wavelength is 0.53 μm (frequency-doubled 1.05 μm). Temporally, the pulse is flat topped with rise and fall times of less than 100

psec and a 1 nsec duration. The experimental intensities quoted here are the average laser power divided by the illuminated area as determined from x-ray micrographs (x-ray energy of $\sim$ 1–1.5 keV). The beam diameter is the average FWHM of the x-ray intensity. Localized regions of higher intensities, due to beam nonuniformities[14] or filamentation, may be present. However, recent work[15] indicates that filamentation will produce only a modest enhancement, if any, of the SRS level. The thickness of the CH foil was chosen by use of two-dimensional hydrodynamic simulations with the code Lasnex,[16] so that 200 psec into the flat part of the laser pulse, the electron density is near resonance ($n_c/4$) for the Raman[5] and $2\omega_{pe}$ instabilities.[17]

The targets were irradiated at 27° from normal incidence with the focus in front of the target. A mask at the center of the lens and the chromatic aberration of the $f/4$ focusing lens caused the 0.53-μm light to focus in a region free from residual 1.05-μm light.[12] However, some 1.05-μm light scatters from the target support stalk, and is visible in the spectral data.

Two time-resolved optical spectrometers with absolute timing fiducials measured the up- and down-shifted forward Raman light. The two instruments are separated by 15°, and are 39° and 27° from $\mathbf{k_0}$, respectively. The angle between the spectrometers and the target normal was varied from 153° to 170°, with no observed differences. Typical data are shown in Fig. 2. The forward-scattered, up-shifted spectrum is clearly resolved at an estimated fluence of 0.1 J/sr. Also in Fig. 2 is the forward-scattered down-shifted light taken
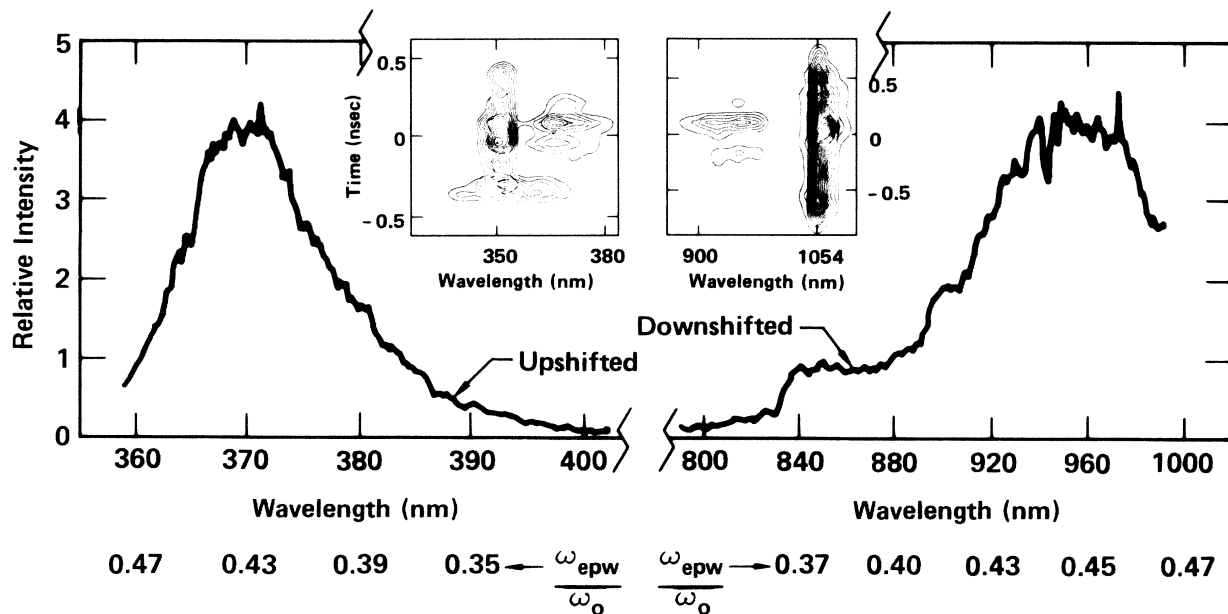
FIG. 2. Up- and down-shifted spectra from Raman forward scattering. Time-integrated from -0.3 to 0.5 nsec (laser pulse runs from -0.5 to 0.5 nsec, as shown on contour plots of data at top of figure). Up-shifted spectra shown $\sim$ 10 times actual height. Residual 1.05-μm light, and $\frac{3}{2}$ doublet near 350 nm, not shown on graph.

on the same shot, as well as contour plots of the actual streak-camera data.

Below the wavelength scale in Fig. 2, we have indicated the electrostatic wave frequency inferred from $\omega_s = \omega_o \pm \omega_{epw}$ for the up- (+) and down-shifted (−) spectra. By a squaring of ω_{epw} (the Bohm-Gross term is negligible here), it is readily seen that the up- and down-shifted scattered light are both originating in the same density region ($0.14 \leqslant n/n_c \leqslant 0.22$). Note that RFS is observed only from relatively high densities. Previous experiments[6] under similar conditions showed that SRS backscattered light occurred over a wider density range, extending to as low as $n/n_c \leqslant 0.1$. The data are consistent with the strong density dependence of the RFS convective gain shown in Fig. 1. They are also consistent with the idea of an enhanced noise source due to the propagation of plasma waves from backward SRS, since the waves at lower densities will suffer increased Landau damping.

We have observed that the RFS emission pulsates rapidly in time (< 100 ps). (These pulsations are too rapid to be visible in the Fig. 2 contour plots.) The up- and down-scattering pulsations correlate approximately, but not exactly, in time. The lack of precise correlation may be due to the 15° spread between the instrumentation.

Four calibrated photodiodes, filtered to look only at down-shifted RFS from below $n_c/4$ ($0.6 \ \mu m < \lambda_s < 1.0 \ \mu m$), measured the absolute level of Raman-scattered light in the forward and backward directions (near 153° and 23° from the laser). Spectroscopy verified that all Raman light emissions were within this range of wavelengths. Typical fluences recorded by the diodes ranged from 2 to 6 J/sr in the forward direction, and 200 to 450 J/sr in the backwards direction, with calibration uncertainties of 30%. We presume that the variations observed are due to variations in laser energy and small changes in the focusing. While there were too few diodes to draw quantitative conclusions regarding the total scattered energy, the backscattered signals are consistent with previous similar measurements[6] where up to 10% of the laser energy appears as SRS backscatter. The measured forward scattering corresponds to an amplification of roughly exp(17) over the thermal level. The thermal level is calculated from Eq. (12) of Seka et al.,[18] with transmission factors of 0.5. This is in reasonable agreement with the gain calculated from Eq. (1). The ratio of the down-shifted energy to the up-shifted energy, measured by the spectrometers, was typically 35. Because of calibration uncertainties, this number should be considered as order of magnitude only. Note too that we have measured this ratio at only the one pair of locations. The ratio reflects the level of damping encountered by the plasma wave propagating between the Stokes and anti-Stokes phase-matching

regions. Thus a more complete measurement of the energies and density scale lengths should yield information on the plasma-wave damping coefficient.[9] In the case of scattering from low densities[19] ($n \ll n_c$), the phase-matching regions can overlap, and the down- to up-shifted ratio can approach unity.

Both Raman backward and forward scattering can produce suprathermal electrons. We measure the x-ray bremsstrahlung from these electrons, as shown in Fig. 3. The hottest component ($T \sim 130$ keV) is consistent, within the experimental uncertainty, with Raman forward scattering at the spectrally inferred density. The heated electrons at a temperature of 22 keV are consistent with those expected from Raman backscattering from an average density $0.12 n_c$, which is similar to previous results.[6, 20]

The x rays were measured with filter-scintillator-photomultiplier detectors. It is well known that the shape of the spectra obtained with such detectors is subject to large uncertainties when the photon energies are > 100 keV, since no K-edge filters exist for this range. The low atomic number and small areal density of these targets produces a very weak bremsstrahlung signal. Furthermore, the shape of the spectra may not be indicative of the electron distribution if the fastest electrons escape from the target without radiating. The data shown in Fig. 3 were obtained on the shot which produced the strongest RFS. Error analysis indicates that the data are not consistent with a factor of 2 smaller superhot temperature. It is difficult to assign an accurate error bar to the upper temperature limit, because of the flatness of the slope. On shots with weaker RFS, which produced weaker but still readable x-ray signals, the best fit to the data varied; however, temperatures in excess of 100 keV are within the error bars. Despite the above caveats concerning the small areal density, we have applied a thick-target bremsstrahlung model to the x-ray data, with the following
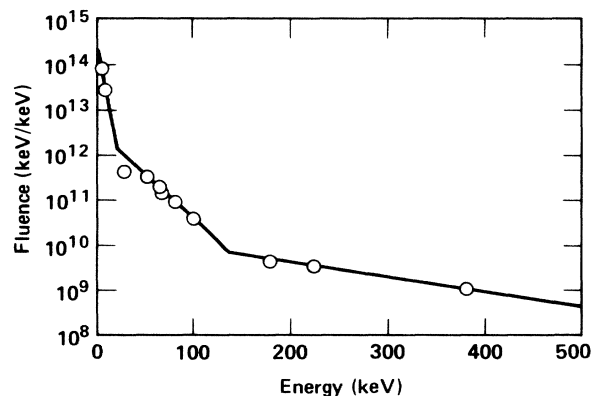
FIG. 3. X-ray spectra showing thermal electrons, heated electrons from Raman backscattering at 22 keV, and those from Raman forward scattering at ~ 130 keV.

results: The energy in hot electrons (22-keV component) is a few percent of the laser energy, while the energy in superhot electrons (130-keV component) is 175 times less. We note the good agreement with the backward and forward, respectively, optical-diode SRS measurements.

The data can be summarized as follows: (1) A superhot ($T > 100$ keV) electron component is measurable when we observe strong (>4 J/sr) RFS; (2) we always observe an up-scattered forward signal at $\omega_o + \omega_{epw}$ whenever down-scattered RFS at $\omega_o - \omega_{epw}$ is observed; (3) the observed spectra support the origin of the upward scattering as the anti-Stokes component produced from the resonant RFS process; (4) at our one pair of observation angles, the up-scattered light is 10–100 times weaker than the down-scattered light.

We consistently observed two anomalies, which are visible on the contour plot in Fig. 2. The $\frac{3}{2}\omega_o$ doublet (attributed to the $2\omega_{pe}$ instability) persists throughout the experiment. We postulate that this is due to the relatively small spot size used here, which results in a two-dimensional, nonplanar plasma. The density near the edge of the laser beam evidently does not drop below $n_c/4$. However, this should not affect our basic conclusions regarding RFS. Second, we observe, early in time ($t = -0.35$ ns), a broad-band, narrow-in-time (~ 100 psec) pulse. This pulse does not fit our explanation for the remainder of the data, since part of it is too blue shifted to be associated with an SRS anti-stokes line. No corresponding down-shifted signal was observed; this is not surprising since the plasma is still overdense to long-wavelength light at this early time. While we do not know the origin of this pulse, it may be associated with two-plasmon decay.

In summary, we have observed the up-shifted line of Raman forward scattering in a laser-plasma interaction experiment. We have measured sufficient up-shifted energy that there is no reasonable doubt that the upward shift is due to Raman forward scattering as opposed to enhanced Thomson scattering.[21] The upward shift is characteristic of Raman forward scattering, and therefore is strong evidence for the presence of that instability.

[1]H. Figueroa *et al.*, Phys. Fluids **27**, 1887 (1984).

[2]W. C. Mead *et al.*, Phys. Fluids **26**, 2316 (1983).

[3]K. Tanaka *et al.*, Phys. Rev. Lett. **48**, 1179 (1982); C. C. Shepard *et al.*, Bull. Am. Phys. Soc. **28**, 1058 (1983); D. Phillion *et al.*, Phys. Fluids **25**, 1434 (1982), and Phys. Rev. Lett. **49**, 1405 (1982); see also A. A. Offenberger *et al.*, Phys. Rev. Lett. **49**, 371 (1982); R. G. Watt, *et al.*, Phys. Rev. Lett. **41**, 170 (1978); R. G. Watt and Z. A. Pietrzyk, Appl. Phys. Lett. **37**, 1068 (1980).

[4]C. S. Liu *et al.*, Phys. Fluids **17**, 1211 (1974); J. F. Drake *et al.*, Phys. Fluids **17**, 778 (1974); D. W. Forslund, J. M. Kindel, and E. L. Lindman, Phys. Fluids **18**, 1002 (1975); R. P. Drake *et al.*, Phys. Rev. Lett. **53**, 1739 (1984).

[5]K. Estabrook and W. L. Kruer, Phys. Rev. Lett. **53**, 465 (1984), and references within.

[6]R. E. Turner *et al.*, Phys. Rev. Lett. **54**, 189 (1985).

[7]K. G. Estabrook and W. L. Kruer, Phys. Fluids **26**, 1892 (1983).

[8]C. Joshi *et al.*, Phys. Rev. Lett. **47**, 1285 (1981).

[9]E. A. Williams, to be published.

[10]T. W. Johnston, private communication.

[11]P. Koch and E. A. Williams, Phys. Fluids **27**, 2346 (1984); D. M. Villeneuve and H. A. Baldis, to be published.

[12]*1982 Laser Program Annual Report* (Lawrence Livermore National Laboratory, Livermore, California, 1983), Sect. 2.

[13]J. Holtzrichter, Nature (London) **316**, 309 (1985).

[14]K. R. Manes and W. W. Simmons, J. Opt. Soc. Am. A **2**, 528 (1985).

[15]H. C. Barr *et al.*, Phys. Rev. Lett. **56**, 2256 (1986).

[16]G. B. Zimmerman and W. L. Kruer, Comments Plasma Phys. Controlled Fusion **2**, 51 (1975).

[17]A. B. Langdon *et al.*, Phys. Rev. Lett. **43**, 133 (1979).

[18]W. Seka *et al.*, Phys. Fluids **27**, 2181 (1984).

[19]C. Clayton *et al.*, Phys. Rev. Lett. **54**, 2343 (1985).

[20]R. P. Drake *et al.*, Phys. Rev. Lett. **53**, 1739 (1984), and to be published.

[21]A. Simon and R. W. Short, Phys. Rev. Lett. **53**, 1912 (1984).